# Influence of Austenite and Martensite Strength on Martensite Morphology

R. G. DAVIES AND C. L. MAGEE

The martensite morphology and austenite flow strength have been determined in a variety of ferrous alloys chosen so that the austenites were paramagnetic, ferromagnetic, substitutional strengthened, and interstitial strengthened. It is demonstrated that two of the most important variables in determining the habit plane (and thus morphology) of martensite in a given alloy are the resistances to dislocation motion in austenite and in ferrite (*i.e.*, martensite). In the wide variety of alloys where martensite with a $\{259\}_\gamma$ habit plane was observed, the austenite flow strength at $M_s$ is greater than 30,000 psi. At lower austenite strengths, either $\{225\}_\gamma$ or $\{111\}_\gamma$ habit planes are found depending on the resistance to dislocation motion in ferrite. Thus, $\{225\}$ martensites are not always found as part of the spectrum between $\{111\}$ and $\{259\}$ martensites but only in the cases (*e.g.*, interstitial strengthening) where ferrite is preferentially strengthened relative to austenite. All of the observations are consistent with the idea that the habit plane observed in a given alloy is the one involving the minimum plastic work for the lattice invariant shear.

In ferrous alloys there are three identifiable types of martensite characterized by habit planes that can be conveniently denoted as $\{259\}_\gamma$, $\{225\}_\gamma$, and $\{111\}_\gamma$.*

*These three are really nominal habit planes summarizing a large number of result.[1] By {259} we refer to habit planes normals near the center of the stereographic triangle,[2] {225} refers to those on the symmetry line near {225}[3] and {111} those near {111}.[4,5]

Martensites with $\{225\}_\gamma$ and $\{259\}_\gamma$ habit planes form as essentially individual plates while the martensites with $\{111\}_\gamma$ habit planes form as packets of highly dislocated platelets or laths.[6] The packet morphology is quite different from that of plates and it is also possible to distinguish between the plate martensites upon the basis of their appearance under a light microscope.[7] $\{259\}$ martensite has a lens shape, exhibits a midrib, is internally twinned and forms by a "burst" to produce the characteristic zig-zag pattern of plates. The plates of $\{225\}$ martensite do not form in a burst, do not have a clearly defined midrib but are internally twinned.[8] Thus, all the available evidence indicates that habit planes can be inferred from morphological observation—a fact we rely upon heavily in the present work. Our own limited habit plane measurements have confirmed the previous correlations and so in the present text we are, for convenience, using habit plane designations for morphological observations.

The various martensites have been documented in a variety of alloys; viz.: $\{259\}$ martensite in Fe-29.5 to 34 pct Ni, and Fe-1.4 to 2.0 pct C.[3] $\{225\}$ martensite in some stainless steels,[9,10] Fe-Ni-Mn-C,[7] and Fe-0.9 to 1.4 pct C alloys;[3] and $\{111\}$ martensite in Fe-10 to 28 pct Ni[11] and Fe-0 to 0.55 pct C alloys.[5] It has also been noted that $\{111\}$ martensite is always cubic, while in carbon containing alloys both $\{259\}$ and $\{225\}$ martensites are tetragonal.[12,13] The major intent of the present work is to uncover the reasons behind the formation of different martensites in different alloys.

R. G. DAVIES and C. L. MAGEE are with the Metallurgy Department, Scientific Research Staff, Ford Motor Company, Dearborn, Mich.

Manuscript submitted November 12, 1970.

Previously we showed that austenite ferromagnetism is a necessary but not sufficient condition for the formation of $\{259\}$ martensite in zero carbon Fe-Ni and Fe-Ni-Co alloys.[14] In these alloys, $\{259\}$ martensite forms when the Curie temperature is sufficiently greater than $M_s$ (*e.g.*, at above 29.5 pct Ni in the Fe-Ni alloys). It was suggested that the correlation of martensite habit plane with ferromagnetism arises because of "Invar strengthening". [Ferromagnetic austenites, which exhibit Invar characteristics, show an enhanced temperature dependence of the flow stress below their Curie temperatures, $\theta_c$.[15]] As the flow stress of the parent austenite increases, the work required to form $\{111\}$ martensite increases, until above some critical austenite flow stress $\{259\}$ martensite would require less energy to form.[14]

In the present work we have tested and extended this idea of the relative amounts of plastic work controlling the morphology of martensite through examination of solid solution strengthening by both interstitial and substitutional alloy elements. We will show upon the basis of certain reasonable assumptions concerning the lattice invariant strains required by each type of martensite that the strengths of the austenite and martensite phases determine the conditions under which each type of martensite will form.

## 1) EXPERIMENTAL PROCEDURE

All the alloys, except those containing platinum and palladium, were prepared as 5 lb vacuum-cast ingots; 0.25 pct Ti was added to the zero carbon alloys to combine with any residual carbon. The ingots were hot rolled at 1000°C to $\frac{1}{4}$ in. diam rod which was subsequently homogenized at 1250°C for 2 hr. The Fe-Pt and Fe-Pd alloys were electron beam melted 20 g buttons which were homogenized for 65 hr at 1250°C.

Both the $M_s$ and $\theta_c$ were obtained from a simple quartz dilatometer which utilized a linear variable differential transformer and a search coil. The apparatus and the means of distinguishing between $M_s$ and $\theta_c$ have been described in detail previously.[14] Both $M_s$ and $\theta_c$ are accurate to ±5°C.

The temperature dependence of the flow stress was obtained from compression tests, upon samples $\frac{1}{4}$ in. diam by $\frac{1}{2}$ in. long at an Instron crosshead rate of 0.02 in. per min, by the temperature change technique.[15] This method has the advantage of utilizing only one sample for the whole temperature range. Heating of the samples for high temperature tests was by means of a radiation furnace.

## 2) RESULTS

In order to pursue the idea that austenite strength governs the martensite morphology many alloys whose compositions, observed $\theta_c$, $M_s$, and morphology are given in Table I, were studied. These alloys can be conveniently divided into the following four groups:

a) Ferromagnetic Austenites—Alloys 1 to 3 in Table I. Fe-Ni-Cu alloys were prepared since the micrographs shown by Hornbogen and Meyer[16] demonstrate lenticular midribbed martensite in similar alloys. Copper, being essentially the same size as iron and nickel, should not give rise to solid solution strengthening. Thus lenticular martensite is only expected on the present viewpoint if the alloys are ferromagnetic. Similarly Efsic and Wayman[17] have shown {259} martensite in a disordered (quenched from 1000°C) Fe-24.5 at. pct Pt alloy while published data indicates this alloy is paramagnetic.[18] Additional results on the alloys used in our previous investigation, which was concerned exclusively with ferromagnetism and martensite morphology,[14] will be presented.

b) Paramagnetic Substitutional Strengthened Austenites—Alloys 4 to 11 in Table I. For this part of the study Fe-Ni alloys containing aluminum and molybdenum were utilized since both aluminum and molybdenum have been shown to be good austenite strengtheners.[19,21] In addition an Fe-Pd alloy was prepared since palladium, being a large atom compared to iron, substantial solution strengthening should result; this alloy will also indicate whether our results are general and apply to alloys other than those based upon Fe-Ni.

c) Paramagnetic Interstitial Strengthened Austenites—Alloys 12 to 16 in Table I. These alloys are based upon Fe-Ni-2 Mn*-C with the nickel and carbon contents balanced so as to give an approximately constant $M_s$ of −15°C.

*2 pct Mn was used to depress $\theta_c$ well below $M_s$.

d) Ferromagnetic Interstitial Strengthened Austenites—Alloys 17 to 19 in Table I. These alloys were prepared specifically to test the correlation between Zener ordering temperature, $T_z$, and martensite morphology, that is observed in paramagnetic Fe-C and Fe-Ni-C alloys;[12,13] if $T_z > M_s$ packet (*i.e.*, {111}) martensite results while if $T_z < M_s$ plate martensite forms.

The results for the first three alloy series will be presented under the major subheadings of morphology and strength. Data obtained from the alloys made to test the correlation of Zener ordering and martensite morphology are given last.

Table I. Composition, Transition Temperatures and Martensite Habit Planes of Alloys Studied

| Alloy No. | Composition* Wt Pct, Bal. Fe | $\theta_c$, °C | $M_s$, °C | Habit Plane |
|---|---|---|---|---|
| 1 | 25Ni 8Cu | 120 | 2 | {259} |
| 2 | 25Ni 9Cu | 175 | − 23 | {259} |
| 3 | 53.1Pt (24.5 At. pct) | 70 | − 3 | {259} |
| 4 | 34Pd (21 At. pct) | – | 187 | {259} |
| 5 | 18Ni 10Mo | – | 35 | {111} |
| 6 | 20Ni 10Mo | – | −180 | {259} |
| 7 | 30Ni 6.2Al | −110 | −115 | {259} |
| 8 | 28Ni 6.2Al | – | − 40 | {259} |
| 9 | 26Ni 6.2Al | – | 35 | {259} |
| 10 | 25Ni 6.2Al | – | 82 | {111}-{259} |
| 11 | 25Ni 5.0Al | – | 95 | {111} |
| 12 | 25Ni 2Mn | – | − 5 | {111} |
| 13 | 21.5Ni 2Mn 0.18C | – | − 9 | {225} |
| 14 | 18Ni 2Mn 0.37C | – | − 20 | {225} |
| 15 | 14.5Ni 2Mn 0.55C | – | − 28 | {225}-{259} |
| 16 | 11Ni 2Mn 0.71C | – | − 28 | {225}-{259} |
| 17 | 20Ni 30Co 0.20C | 445 | 165 | {259} |
| 18 | 19Ni 30Co 0.20C | 420 | 217 | {259} |
| 19 | 16Ni 30Co 0.42C | 385 | 280 | {259} |

*Nominal composition, although analysis for substitutional elements in several alloys showed less than 0.1 pct deviation from nominal; all carbon contents determined analytically.

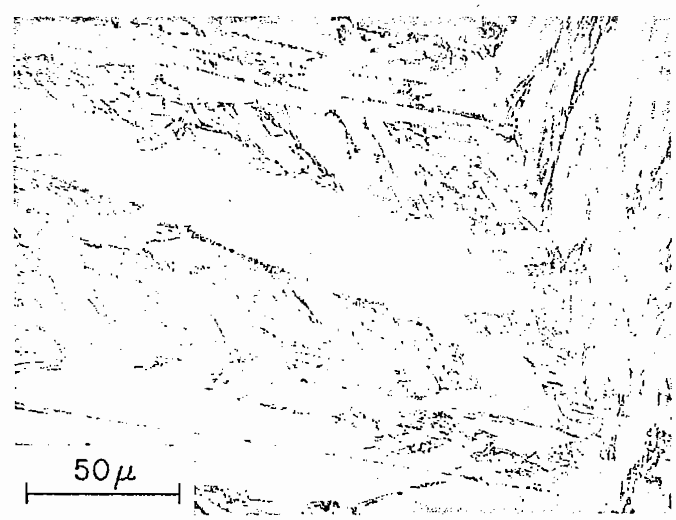


Fig. 1—Midribbed martensite in Fe-25 Ni-8 Cu alloy.

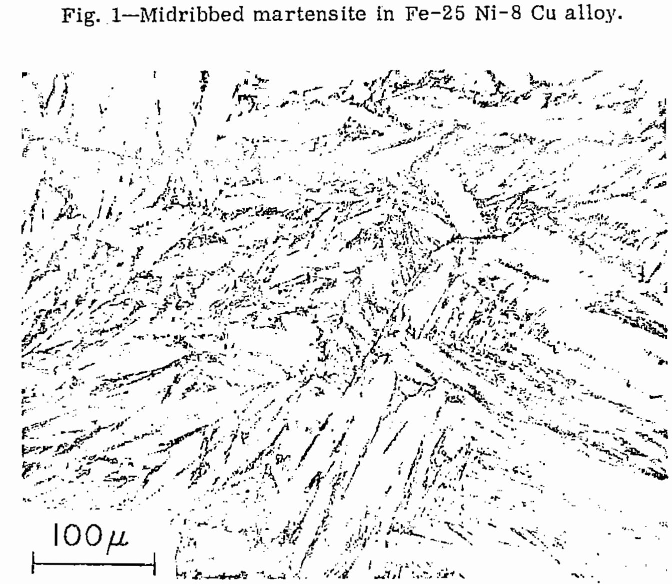


Fig. 2—Midribbed martensite in Fe-34 Pd alloy.

### 2.1) Morphology

a) Ferromagnetic Austenite. As indicated in Table I, $\theta_c$ for the Fe-Ni-Cu alloys is considerably above $M_s$ and therefore the observation of {259} martensite as shown in Fig. 1 is consistent with our earlier work on Fe-Ni and Fe-Ni-Co alloys.[14,21] It should be noted that while copper depresses $M_s$ it raises $\theta_c$ substantially; $\theta_c$ for Fe-25 Ni is approximatdly 0°K. Similarly, and contrary to published work,[18] the platinum alloy (disordered by quenching from 1000°C into brine) is ferromagnetic prior to the martensitic transformation. Thus the observation of {259} martensite in this alloy is not surprising.

b) Paramagnetic Substitutional Strengthened Austenites. The results presented in Table I for these alloys show that it is possible to obtain {259} martensite in carbon-free paramagnetic alloys. Fig. 2 is a micrograph of {259} martensite in the Fe-Pd alloy while Fig. 3 shows the {259}, {111}, and mixtures of these two martensites in the Fe-Ni-Al alloys; a similar structural transition was noted in the Fe-Ni-Mo alloys.

For both the ferromagnetic and paramagnetic substitutional strengthened alloys the morphological transition is from {111} to {259} martensite.

c) Paramagnetic Interstitial Strengthened Austenites. In contrast to the results presented above, Fe-Ni-Mn-C alloys show two morphological transitions: 1) a {111} to {225} martensite which takes place at a carbon content of less than 0.17 pct and 2) a {225} to {259} martensite which occurs at a composition of approximately

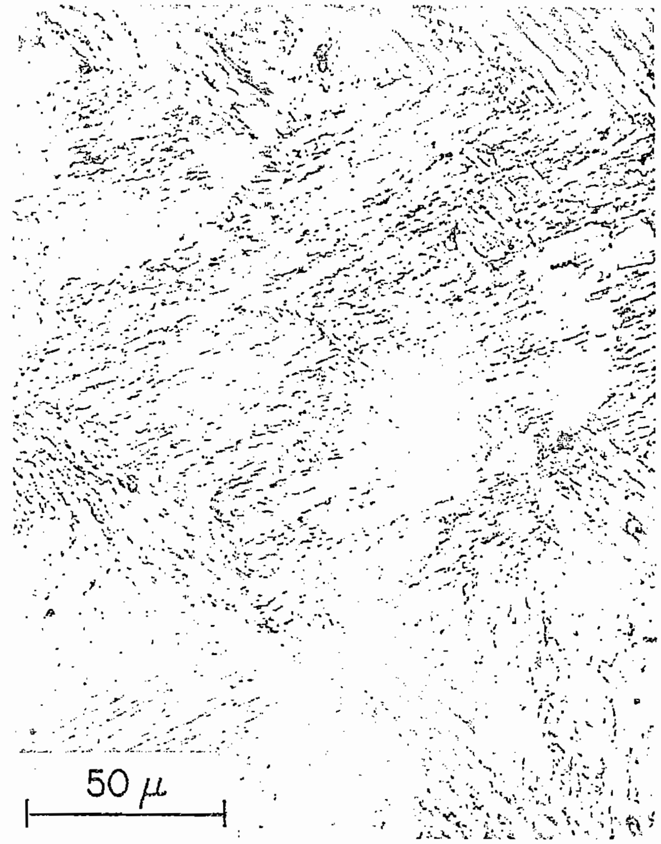


(b)

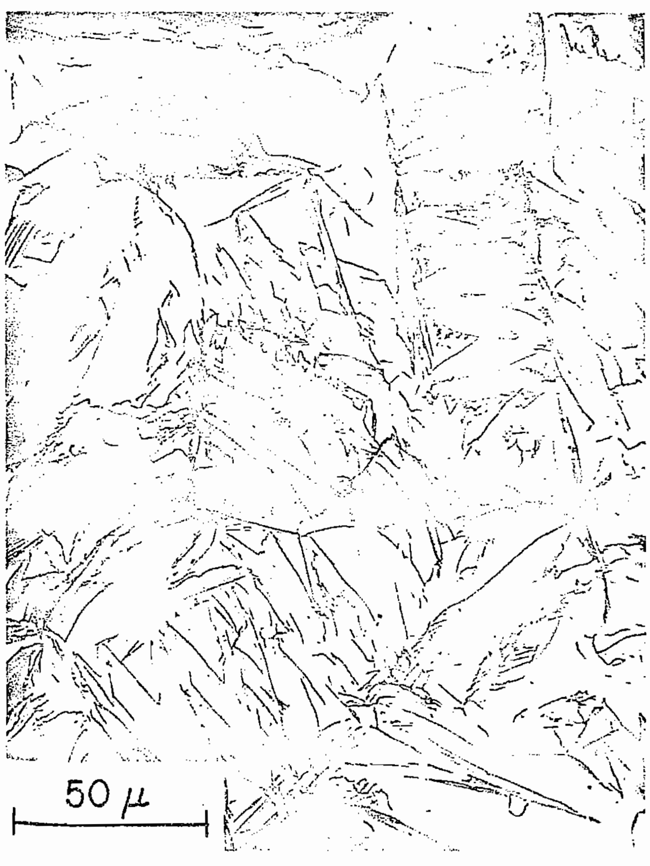


(a)

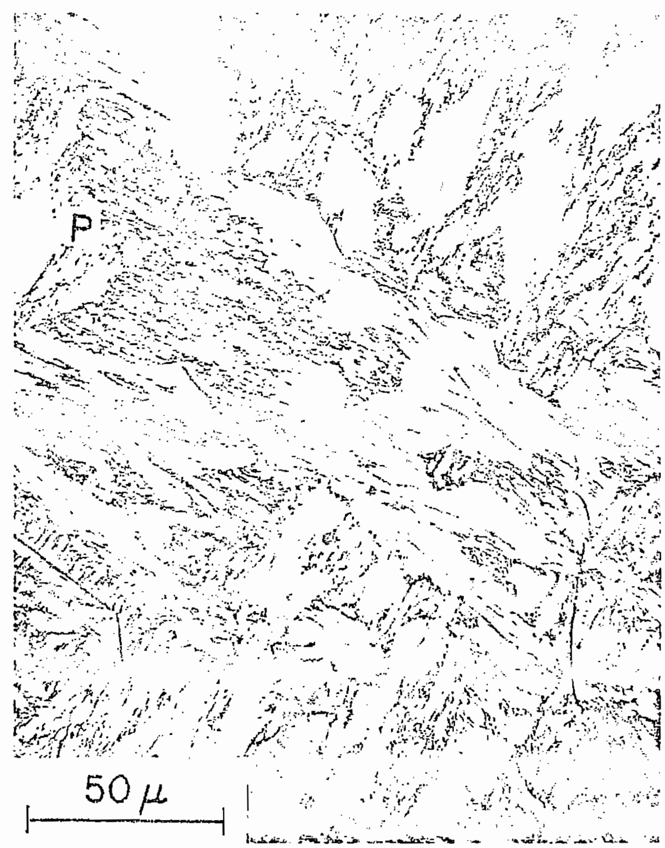


(c)

Fig. 3—Martensites in Fe-Ni-Al alloys; (a) {259} martensite in Fe-28 Ni-6 Al; (b) {111} martensite in Fe-25 Ni-4 Al; and (c) mixed {259}-{111} martensites in Fe-25 Ni-6 Al alloy.

0.5 pct C. In this series the {225} to {259} transition is very smeared. Although some {259} martensite is present at 0.59 pct C, the 0.71 pct C alloy contains appreciable {225} martensite along with {259} martensite. Fig. 4 shows the {111}, {225}, and {259} martensites observed in this alloy series.

### 2.2) Strength of Austenite

The flow stresses (by the temperature change technique and at a strain rate of $10^{-3}sec^{-1}$) of all the alloys have been measured as a function of temperature; only representative results will be presented in the following sections. It is recognized that martensite plates are reported to grow at rates between $10^{-2}$ (Ref. 22) and $10^{4}$ (Ref. 23) cm per $sec^{-1}$, and if it is assumed that the 0.2 martensitic shear is accommodated over a distance of $10^{-3}$ cm in front of the growing plate, then effective strain rates of 1 to $10^{6}$ $sec^{-1}$ are obtained. Thus, the measured flow stresses cannot directly correspond to the stresses relevant during the growth of a martensite plate. Also the critical stresses that should be important in determining the habit plane are probably those for dislocation motion on a given plane or for a specific dislocation interaction. Nevertheless, it is not unreasonable to look for a correlation between the measured flow stress and the habit plane transitions.

The austenite flow stress begins to decrease at temperatures 20° to 50°C above $M_S$ due to the stress induced formation of martensite.[24] Therefore it is nec-

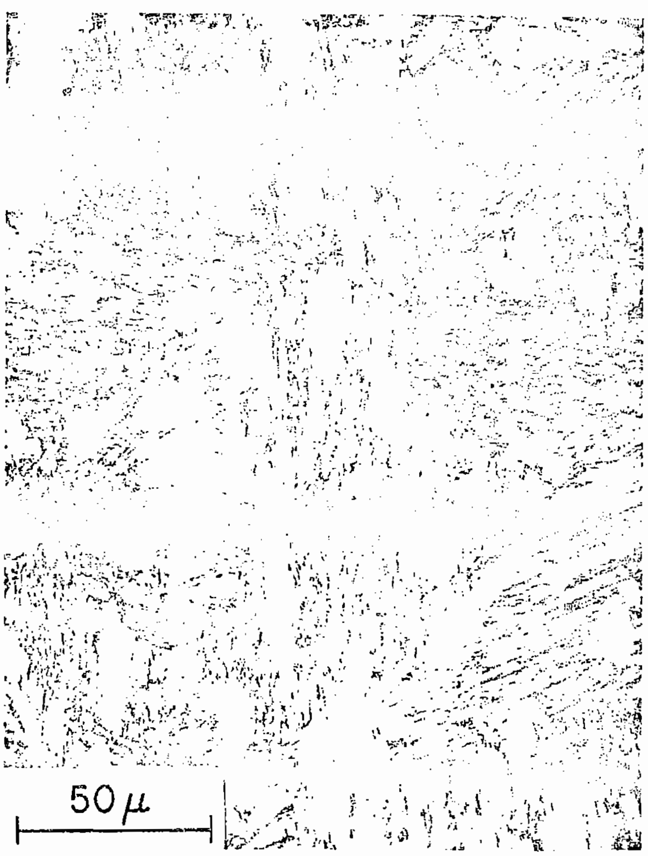


(a)

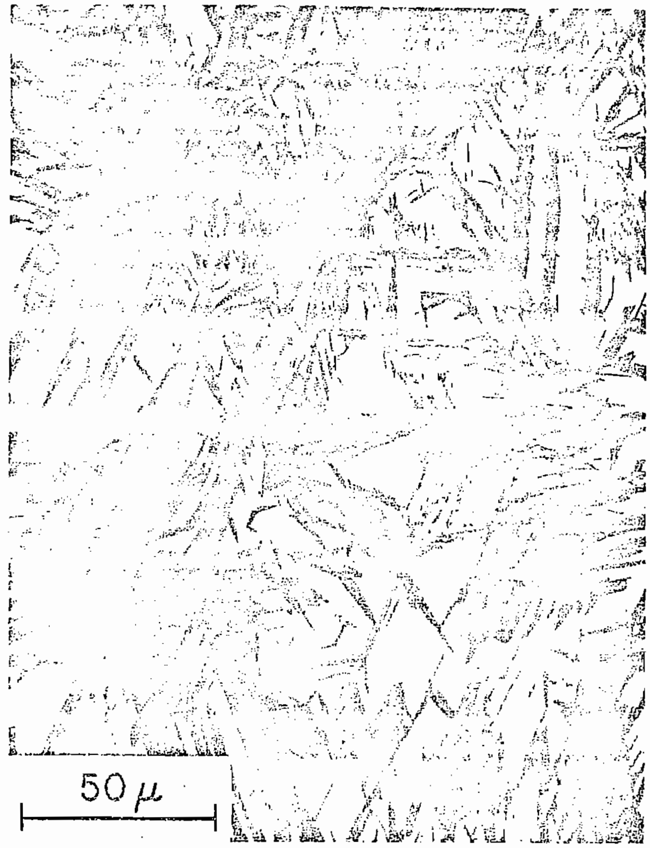


(b)

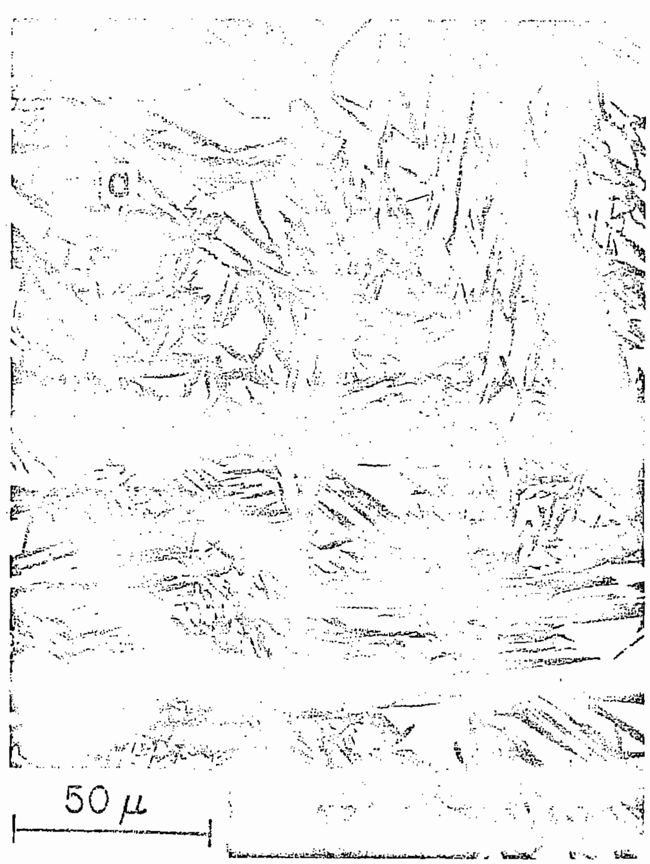


(c)

Fig. 4—Martensites in Fe-Ni-2 Mn-C alloys; (a) {111} martensite in zero carbon alloy; (b) {225} martensite in 0.37 pct C alloy; and (c) {259} martensite in 0.71 pct C alloy; note zig-zag groups of midribbed plates at "α" indicative of {259} martensite.[7]

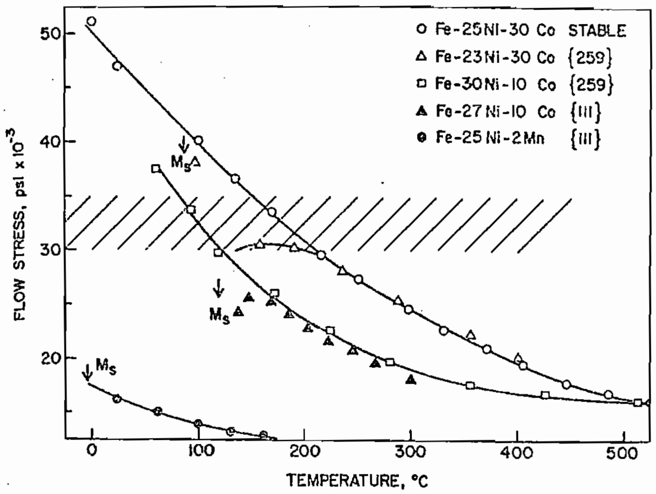


Fig. 5—Flow stress vs temperature for several ferromagnetic (and a paramagnetic) austenitic alloys. The cross-hatching divides {259} (above) from {111} martensite in each alloy series.

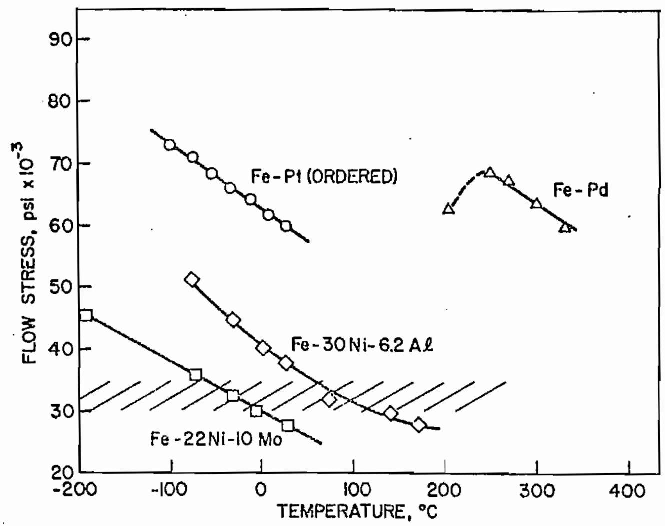


Fig. 6—Flow stress vs temperature for substitutional strengthened austenitic alloys. Results for Fe-22 Ni-10 Mo and 30 Ni-6.2 Al hold for all alloys in their respective series, Table I. Cross-hatching refers to appearance of {259} martensite.

essary to extrapolate from higher temperatures in order to obtain a value of the flow stress at $M_s$. However, it has been found that the flow stress of austenite is independent of Ni, Co, Mn, and Cu content but dependent upon aluminum and molybdenum content.[19] Thus for the Fe-Ni-6.2 Al and Fe-Ni-10 Mo alloys it was possible to use stable austenites to give a measure of the flow stress at $M_s$ for alloys that did transform to martensite. Experiments on the metastable austenites in these series (well above $M_s$) confirmed that the flow stress was the same as for the stable alloy. Similarly, the production of long range order in the Fe-Pt alloy (annealed 16 hr at 600°C) depresses $M_s$[17,18] and allows flow stress measurements over a wider temperature range; at room temperature the long range ordered specimen had a flow stress ~5000 psi less than that of the quenched (disordered) specimen.

a) Ferromagnetic Austenites. The results for some of the ferromagnetic Fe-Ni-Co and a paramagnetic Fe-Ni-Mn alloy are shown in Fig. 5. Using the figure, a correlation between martensite habit plane and austenite flow stress can be noted. If the flow stress of the austenite, extrapolated to $M_s$, is greater than 30 to 35,000 psi then {259} martensite forms, for example in the alloys Fe-23 Ni-30 Co and Fe-30 Ni-10 Co. For both the Fe-Ni-Cu alloys the flow stress at $M_s$ was in excess of 35,000 psi. However, if the flow stress is less than 30,000 psi, as for Fe-27 Ni-10 Co and Fe-25 Ni-2 Mn alloys, {111} martensite forms.

b) Paramagnetic Substitutional Strengthened Austenites. Fig. 6 shows the temperature dependence of the flow stress for the substitutional strengthened Fe-Ni-6.2 Al, Fe-Ni-10 Mo, and Fe-Pd alloys. Comparing the flow stresses in Fig. 6 with the morphologies and $M_s$'s indicated in Table I it can be seen that if, at $M_s$ the austenite flow stress exceeds 30 to 35,000 psi, {259} martensite is observed. For example the Fe-18 Ni-10 Mo alloy would have a flow stress at $M_s$ (+35°C) of 27,000 psi and form {111} martensite, while Fe-20 Ni-10 Mo has a flow stress at $M_s$ (−180°C) of 45,000 psi and {259} martensite is formed. Similarly it can be calculated (knowing the strength of Fe-Ni-6.2 Al) that the flow stress at $M_s$ for the Fe-25 Ni-5 Al alloy is below 30,000 psi and {111} martensite is again observed.

The data for the Fe-Pt alloy also is included in Fig. 6, although the alloy is ferromagnetic. It is clear that even in the absence of "Invar strengthening" the large platinum atom would strengthen the austenite lattice sufficiently so as to promote {259} martensite. Thus, the correlation between habit plane and ferromagnetism found in Fe-Ni-Co alloys[14] is not expected in the Fe-Pt system.

c) Paramagnetic Interstitial Strengthened Austenites. The flow stress at $M_s$ for the Fe-Ni-Mn-C alloys as a function of carbon content is shown in Fig. 7. Again the appearance of {259} martensite (only seen at wt pct C > 0.5) coincides with an austenite flow stress of ~30,000 psi, at lower flow stresses, {111} and {225} forms. In contrast to these alloys, Fe-Ni-C alloys ($M_s \simeq -35$°C) which have been widely studied[3,13,25] do not show a habit plane transition with increasing carbon content. This is because all the alloys

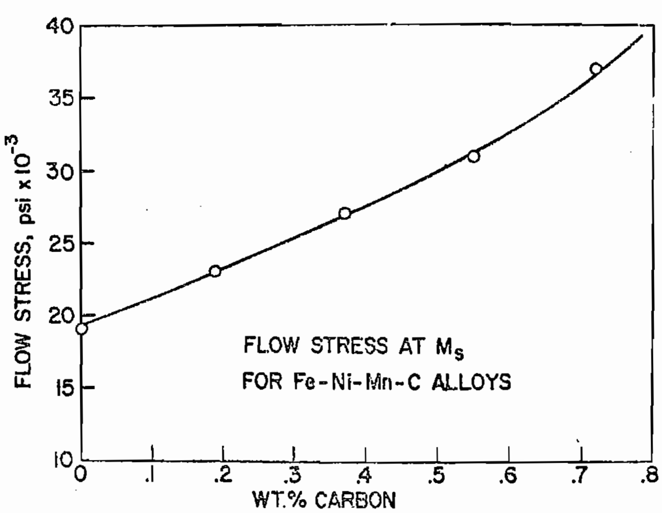


Fig. 7—Flow stress, extrapolated to $M_s$, for the interstitial strengthened paramagnetic austenitic alloys, numbers 12 to 16, Table I.

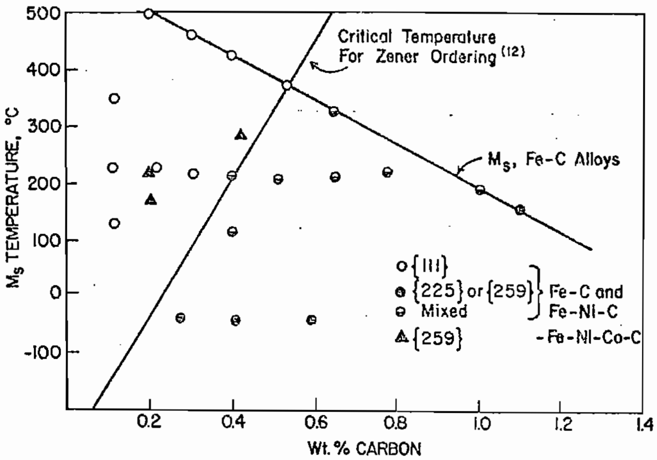


Fig. 8—Influence of $M_s$, and carbon content upon martensite morphology; data for Fe-C and Fe-Ni-C alloys from Ref. 13.

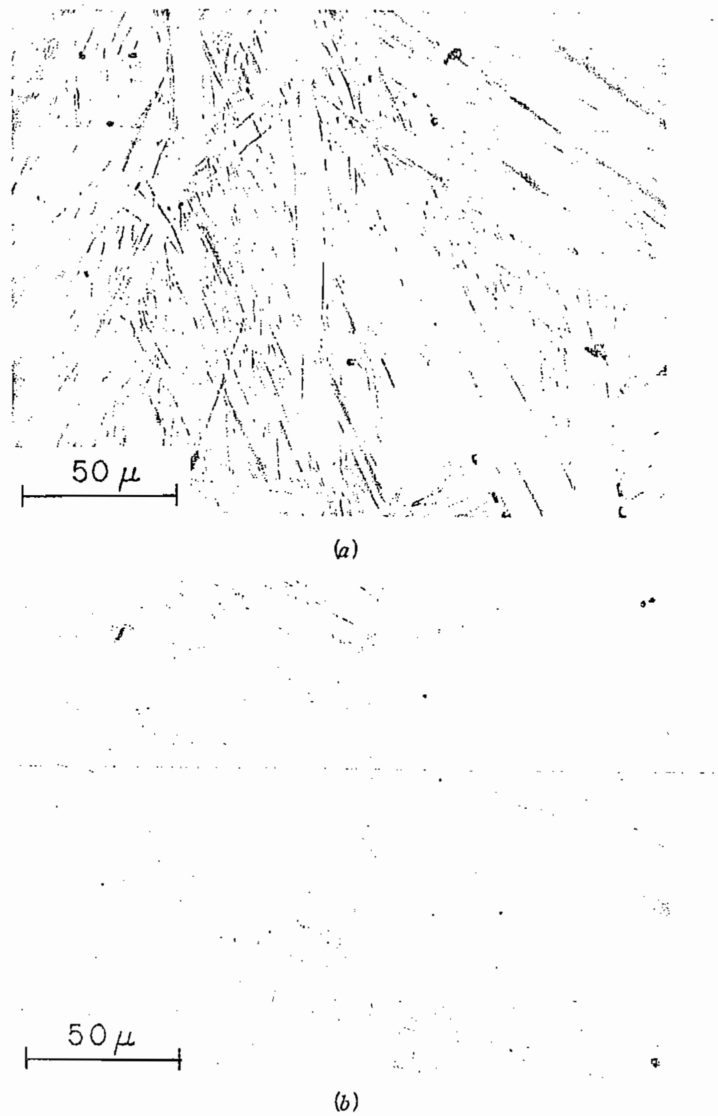


Fig. 9—Midribbed martensite in (a) Fe-16 Ni-30 Co-0.42 C, and (b) Fe-19 Ni-30 Co-0.2 C alloys.

have a flow stress at $M_s$ greater than 30,000 psi and thus form {259} martensite. In low carbon alloys, (*i.e.*, Fe-31 Ni), the strength is attained through ferromagnetic strengthening, while in paramagnetic austenites there is sufficient carbon strengthening.

d) Ferromagnetic Interstitial Strengthened Austenites. As stated earlier and as shown in Fig. 8, there is a reasonable correlation between the Zener ordering temperature of the martensite, $T_z$, and the martensite morphology for paramagnetic Fe-C and Fe-Ni-C alloys. In order to test this correlation more critically, alloys with $M_s > T_z$ and with additional austenite strengthening (by ferromagnetism) were studied—alloys 17 to 19 in Table I. An X-ray diffraction study of the 0.4 wt pct C alloy showed that the martensite was cubic as-quenched consistent with $M_s > T_z$. Fig. 9 shows that the martensite in these alloys consists of midribbed lenticular plates denoting a {259} habit plane. The results, also indicated in Fig. 8, show that the morphology does not correlate with $T_z$ for these alloys. This result also indicates that the Zener disordering occurs after the lattice invariant shear (which presumably takes place at the interface) because twinning is suppressed by a cubic array of interstitials[26] but not by the tetragonal array[27] produced by the Bain strain.

The results for these alloys suggest that the previous correlation of habit plane with Zener ordering is fortuitous; it is probable that the effect of carbon content and temperature on the flow stress of the austenite again governs martensite morphology.

## 3) DISCUSSION

### 3.1) The Hypothesis of Lattice Invariant Shears

The results for all the alloys studied show that strong austenite (flow stress at $M_s$ > 30 to 35,000 psi) transforms to {259} martensite while weaker austenite forms {111} martensite in zero carbon alloys and {225} or {111} martensite in carbon containing alloys. The correlation of a transition martensite morphology at a critical austenite flow stress in the zero carbon ferromagnetic alloys indicates that the strength of the austenite alone can determine the martensite habit plane. (The strength of the resultant martensite is independent of whether the austenite was ferro- or paramagnetic or of whether the habit plane is {111} or {259}.)[11]

We previously proposed that {111} martensite can only result when plastic deformation of austenite occurs in place of some twinning in martensite.[14] We will now extend this earlier suggestion by making assumptions as to the nature of the lattice invariant shears that take place during the formation of the different types of martensite. By applying the premise that martensite forms with the habit plane requiring the least plastic work, we are able to rationalize the formation of the different types of martensite in various alloys.

The proposed lattice invariant shears for the various habit planes are summarized in Table II. These are reasonable shears since: a) for {259} martensite all theories so far proposed assume that the lattice invariant shear is only twinning in the martensite.*[3,28]

*Even when only partially twinned plates are observed,[29] the habit plane appears to be determined by the twinned central region.

b) To account for {225} martensite Acton and Bevis,[30] and Ross and Crocker[31] have developed generalized crystallographic theories that allow independent of one another slip in austenite and twinning in martensite. Bowles and Dunne[32] have suggested that {225} martensites involve "accommodation" shears in austenite

Table II. Proposed Lattice Invariant Shears for the Various Martensite Habit Planes

| Martensite Habit Plane | Accommodation in Martensite | Accommodation in Austenite |
|---|---|---|
| {111} | slip | slip |
| {225} | twinning | slip |
| {259} | twinning | – |

along with twinning in martensite. Further support for this twinning assumption is that {225} martensites are observed to be internally twinned;[3,8] c) for {111} martensite, the assumption of slip in both austenite and martensite is reasonable, since a characteristic of these martensites is their extremely high dislocation density (~$10^{12}$ lines per sq cm) (Ref. 12) with few, if any, twins, and our observation that {111} martensite only forms in soft austenites.

3.2) Relative Strength of Austenite and Ferrite

With these lattice invariant shears it is possible to understand why we have not observed {225} martensite in the ferromagnetic austenites or the substitutional solid solution strengthened alloys, and why it is observed in paramagnetic Fe-Ni-Mn-C alloys. The hypothesized difference in accommodation shears between {111} and {225} martensite is in the deformation mode of the martensite, *i.e.*, slip vs twinning; increasing the slip stress of ferrite alone should result in a transition from {111} to {225} martensite. Fig. 10 is a schematic summary of how the resistance to dislocation motion in ferrite and austenite affects the habit plane of martensite consistent with the postulated shears. These dislocation motion stresses will be influenced by short range interactions such as solid solution hardening and

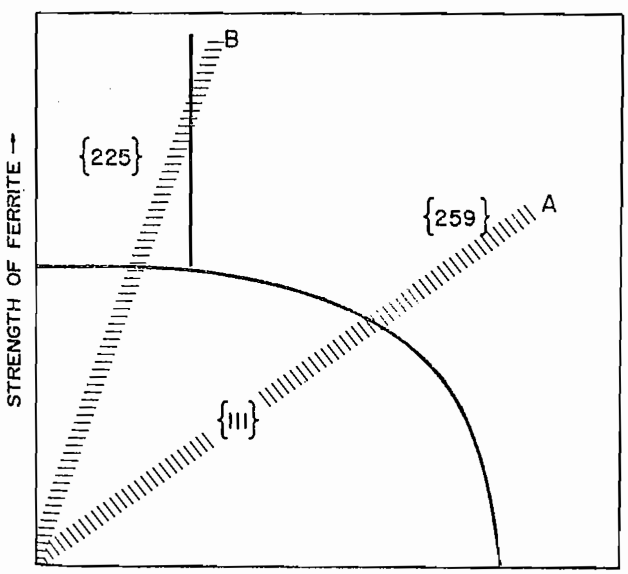


Fig. 10—Schematic representation of the effect of the resistance to dislocation motion in ferrite and austenite upon the martensite habit plane; the regions where each habit plane is favored are separated by solid lines. Path *A* refers to a variable that strengthens austenite and ferrite equivalently. Path *B* refers to a variable that strengthens ferrite more rapidly than austenite.

"Invar strengthening", but probably not by strengthening mechanisms, such as grain size refinement and particle-dislocation interactions, that involve longer range interactions.

Using Fig. 10 it can be qualitatively seen that an element which raises the slip stress of ferrite much faster than that of austenite could result in the formation of {225} martensite. A semiquantitative treatment is possible for the present alloys. The twinning stress for ferrites is ~60,000 psi independent of substitutional solute type or content (neglecting long range order)[33] and the slip stress in austenite and ferrite increases with Al, Mo, and C content as indicated in Table III. With a flow stress of unalloyed austenite and ferrite of ~15,000 psi at room temperature, the substitutional additions lead to strong austenite (>30,000 psi) prior to reaching the ferrite twinning stress. Thus with increasing amounts of substitutional additions the strengths of austenite and ferrite will follow a line near *A* in Fig. 10 and, consistent with observations, only a {111} to {259} habit plane transition is expected.

For the carbon containing alloys the strengths of the austenite and ferrite will follow a line similar to *B* in Fig. 10. The twinning stress of ferrite should be attained by the addition of ~0.1 wt pct C which will have little effect on the austenite flow stress; thus a {111} to {225} martensite transition can be expected at low carbon levels. With more than 0.5 pct C the austenite is strengthened sufficiently to give rise to {259} martensite. Hence, the observed morphological transitions in the Fe-Ni-Mn-C alloys are consistent with the semiquantative calculation and with the hypothesized shears.

The temperature of transformation is also important in determining the ratio of ferrite to austenite flow stress. Ferrites have a slip stress that is much more temperature dependent at low temperatures than that of austenite. Thus, in relatively weak austenites, a very low $M_S$ temperature would favor the formation of {225} martensite. The observations by Reed[36] of {111} martensite in a 304 stainless steel when the transformation temperature was −110°C and {225} martensite when transformed at −196°C, support this idea.

Habit plane transitions can be influenced by other factors besides changes in strength of austenite and martensite. Brook and Entwisle[7] found that replacement of nickel by manganese or chromium in Fe-Ni-0.5 C alloys promoted {225} martensite at the expense of {259} martensite. Manganese and chromium additions will decrease the stacking fault energy[37] without changing the flow stress of the austenite. Thus changes in deformation character (caused by changes in stacking fault energy) seem to affect the {225} to {259} transition. In fact the high carbon {225} martensite observed in certain alloys[38] suggests a second mode for forming

Table III. Values for Solid Solution Strengthening of Ferrite and Austenite

| Alloying Element | Increase in Flow Stress, psi/at. pct: Ferrite | Austenite | Ref. |
|---|---|---|---|
| Al | 4,000 | 1,800 | 34, 19, 20 |
| Mo | 6,000 | 2,000 | 34, 19 |
| C | 140,000 | 4,000 | 34, 35, 20 |

{225} martensite (in addition to the one in Table II) which possibly depends only on stacking faults in austenite. However, stacking fault energy variations play no such role in the {111} to {259} transition since Fe-Ni, Fe-Ni-Al, Fe-Ni-Co, and Fe-Ni-Mo alloys show the transition at similar austenite flow strengths; aluminum and cobalt reduce, while copper and molybdenum raise austenite stacking fault energy.[37]

## 4) CONCLUDING REMARKS

The idea that the martensite forms with the habit plane involving the minimum plastic work bears examination from a mechanistic viewpoint. How, for example, does the martensite recognize the various relative strengths? A possibility is that several sets of embryos with different interfaces—which thus accomplish the lattice invariant shear differently—exist simultaneously. The embryo whose shear would require the least plastic work to be expended, would be the one to grow first and determine the observed martensite habit plane. A more likely mechanistic alternative is that the martensite interface can change character so as to accomplish the lattice invariant shear with the minimum of plastic work. The idea that the nature of the lattice invariant shear can change even during growth is suggested by the midribbed but only partly twinned {259} plates commonly observed.[29] In many instances the morphology away from the center of a {259} plate suggests {111} martensite [for example area $P$ in Fig. 3($c$)] indicating a change in the lattice invariant shear from martensite twinning to slip in both austenite and martensite. This may occur because thickening of a plate takes place more slowly than lengthening and slow rates of straining favor deformation by slip. Alternatively, temperature rises[29] after the initial plate formation could also cause this morphological transition as now, locally, the austenite is weaker.

The general agreement of our experimental results with the hypothesized shears suggests that these shears can serve as a starting point for realistic crystallographic descriptions. In particular, the evidence that the austenite flow strength is a significant factor in determining habit plane strongly suggests that slip in austenite is an intrinsic part of the formation of {111} martensite. Unfortunately, such slip would be inhomogeneous throughout the austenite grain (it would concentrate near the martensite plate) and the crystallographic theory in its present form only treats homogeneous deformations.[31]

The present work also indicates another area into which the present theories must expand. It is to be noted that we have no evidence for a martensite type (*i.e.*, a habit plane) which results from slip in ferrite *alone*. Nonetheless, solutions utilizing slip in ferrite as the only lattice invariant shear can be derived from the recent generalized crystallographic theories[30,31] and even from the original single shear version.[4,28] Their nonappearance suggests that in addition to the amount of plastic work, the structure and mobility of the resulting interface[31] must also be considered in order to determine whether an algebraically possible solution will occur in a real crystal.

Thus, we have emphasized that morphological changes can result from relative differences in the total energy to form the different morphologies in various alloys. In particular, our success in understanding morphology changes on the basis of austenite and ferrite yield strengths indicates that the key energy term is the plastic work associated with the lattice invariant shear.

## 5) CONCLUSIONS

a) High concentrations of the substitutional strengthening elements aluminum or molybdenum when added to Fe-Ni, and palladium or platinum when added to iron result in {259} martensite.

b) In all of these alloys (and in "Invar strengthened" Fe-Ni-Co alloys) it is found that when {259} martensite forms, the austenite flow strength at $M_s$ ($\sigma_{M_s}^{\gamma}$) is greater than 30,000 psi. High resistance to dislocation motion in austenite is thus sufficient to suppress {111} and {225} martensite.

c) In carbon-containing alloys transforming above 100°C, no correlation between habit plane and the Zener ordering temperature is found in strengthened austenites.

d) For $\sigma_{M_s}^{\gamma}$ below 30,000 psi, the habit plane of the martensite is either {111} or {225} depending on the resistance to dislocation motion in the ferrite (*i.e.*, martensite). In particular if the ferrite slip stress is greater than the twinning stress, {225} habit planes are favored. Thus, {225} martensites were not observed in the substitutionally strengthened alloys—just {111} and {259} martensites. However, in carbon-containing alloys where the ferrite twinning stress is attained without substantially strengthening the austenite, {225} martensites were observed.

e) All of these results were consistent with a) reasonable lattice invariant shears, viz.:

{111}—slip in ferrite and austenite
{225}—slip in austenite and twinning in ferrite
{259}—twinning in ferrite

and b) the postulate that among these alternatives, the habit plane observed in a given alloy is the one involving the least plastic work for the lattice invariant shear.

## ACKNOWLEDGMENTS

The authors are grateful to R. Weise for technical assistance and to Drs. H. I. Aaronson and R. H. Richman for critically reviewing the manuscript and to Dr. Y. C. Liu for providing the Fe-Pd alloy.

## REFERENCES

1. J. W. Christian: *Theory of Transformations in Metals and Alloys*, Pergamon Press, London, 1965.
2. J. F. Breedis and C. M. Wayman: *Trans. TMS-AIME*, 1962, vol. 224, pp. 1128-33.
3. C. M. Wayman: *Introduction to the Crystallography of Martensitic Transformations*, MacMillan Company, New York, 1964.
4. W. S. Owen, F. J. Schoen, and G. R. Srinivasan: in *Phase Transformations*, pp. 157-80, ASM Seminar Series, 1970.
5. A. R. Marder and G. Krauss: *Trans. ASM*, 1969, vol. 62, pp. 951-64.
6. G. Krauss and A. R. Marder: *Las Vegas Martnsite Symposium*, to be published in *Met. Trans.*
7. R. Brook and A. R. Entwisle: *J. Iron Steel Inst.*, 1965, vol. 203, pp. 905-12.
8. P. M. Kelly and J. Nutting: *J. Iron Steel Inst.*, 1961, vol. 197, pp. 199-211.
9. J. A. Venables: *Phil. Mag.*, 1962, vol. 7, pp. 35-44.
10. R. Lagneborg: *Acta Met.*, 1964, vol. 12, pp. 823-43.
11. G. R. Speich and P. R. Swann, *J. Iron Steel Inst.*, 1965, vol. 203, pp. 480-85.
12. W. S. Owen, E. A. Wilson, and T. Bell: *High Strength Materials*, V. Zackay,

ed., pp. 167-208, John Wiley and Sons, New York, 1965.
13. C. L. Magee and R. G. Davies: *Acta Met.*, 1971, vol. 19, pp. 345-54.
14. R. G. Davies and C. L. Magee: *Met. Trans.*, 1970, vol. 1, pp. 2927-31.
15. G. F. Bolling and R. H. Richman: *Phil. Mag.*, 1969, vol. 19, pp. 247-64.
16. E. Hornbogen and W. A. Meyer: *Z. Metallk.*, 1967, vol. 58, pp. 297-305.
17. E. J. Efsic and C. M. Wayman: *Trans. TMS-AIME*, 1967, vol. 239, pp. 873-82.
18. A. E. Berkowitz, F. J. Donahoe, A. D. Franklin, and R. R. Steijn: *Acta Met.*, 1957, vol. 5, pp. 1-12.
19. D. J. Dyson and B. Holmes: *J. Iron Steel Inst.*, 1970, vol. 288, pp. 469-74.
20. K. J. Irvine, D. T. Llewellyn, and F. B. Pickering, *J. Iron Steel Inst.*, 1961, vol. 199, pp. 153-75.
21. R. G. Davies and C. L. Magee: *Proc. Second Intern. Conf. on Strength of Metals and Alloys*, 1970, vol. III, pp. 817-21. Sponsored by American Society for Metals.
22. J. M. Marder and A. R. Marder: *Trans. ASM*, 1969, vol. 62, pp. 1-10.
23. R. F. Bunshah and R. F. Mehl: *Trans. AIME*, 1953, vol. 197, pp. 1251-58.
24. J. R. Patel and M. Cohen: *Acta Met.*, 1953, vol. 1, pp. 531-38.
25. P. G. Winchell and M. Cohen: *Trans. ASM*, 1962, vol 55, pp. 347-61.
26. C. L. Magee, D. W. Hoffman, and R. G. Davies: *Phil. Mag.*, to be published.
27. I. Tamura, H. Yoshimura, N. Iwasaki, and M. Ibaraki: *Mem. Inst., Sci. Ind. Res.*, Osaka Univ., 1965, vol. 22, pp. 41-57.
28. M. S. Wechsler, D. S. Lieberman, and T. A. Read: *Trans. AIME*, 1953, vol. 197, pp. 1503-15.
29. R. L. Patterson and C. M. Wayman: *Acta Met.*, 1966, vol. 14, pp. 347-69.
30. A. F. Acton and M. Bevis: *Mater. Sci. and Eng.*, 1969/70, vol. 5, pp. 19-29.
31. N. D. H. Ross and A. G. Crocker: *Acta Met.*, 1970, vol. 18, pp. 405-18.
32. J. S. Bowles and D. P. Dunne: *Acta Met.*, 1969, vol. 17, pp. 677-85.
33. G. F. Bolling and R. H. Richman, *Can. J. Phys.*, 1967, vol. 45, pp. 541-57.
34. N. P. Allen: *Iron and Its Dilute Solid Solutions*, C. W. Spencer and F. E. Werner, eds., pp. 271-308, publ. Interscience, Div. of John Wiley and Sons, New York, 1963.
35. R. G. Davies and R. C. Ku: *Trans. TMS-AIME*, 1966, vol. 236, pp. 1691-96.
36. R. P. Reed: *Acta Met.*, 1962, vol. 10, pp. 865-77.
37. D. Dulieu and J. Nutting: *Iron Steel Inst., (London), Spec. Rept.* no. 86, 1964, pp. 140-45.
38. S. Jana and C. M. Wayman: *Met. Trans.*, 1970, vol. 1, pp. 2825-32.